

The influence of the altered structure zone characteristics after the material jet treatment on the samples stress state during tensility

A.I. Verameichyk  , M.V. Neroda , B.G. Holodar 

Brest State Technical University, Brest, Belarus

✉ vai_mrtm@bstu.by

Abstract. The article investigates the influence of the mechanical characteristics (elasticity module, Poisson coefficient) of the material altered structure zones, which arise after heat treatment by concentrated high-energy impact. For rectangular samples, two forms of the structure formation zone are analyzed - rectangular and crescent-shaped with a zone of processed material in the form of a semicircle. MSC NASTRAN and ANSYS Workbench software packages were used as calculation packages. A computer simulation of the stress-strain state of samples with one or more treated tracks (along the entire length and on the part of the length) under tension was carried out. The influence of the zone size and the distance between them is investigated. An insignificant effect of the distance between the tracks on the voltages has been established. The stress concentration coefficients in the vicinity of the treatment zones are determined. The transverse stresses are studied depending on the mechanical characteristics of the material.

Keywords: mechanical characteristics of the material; stress-strain state; stress concentration coefficient; finite element method; local impact

Acknowledgements. *The work is carried out within the framework of task 3.2.8 of Scientific and Research Work No. 1 "Study of mechanical properties of machine component elements after laser-plasma treatment" of the sub-programme "Electromagnetic, beam-plasma and foundry deformational technologies for material treatment and creation" of the Scientific Research State Programme "Materials study, new materials and technologies" (Belarus).*

Citation: Verameichyk AI, Neroda MV, Holodar BG. The influence of the altered structure zone characteristics after the material jet treatment on the samples stress state during tensility. *Materials Physics and Mechanics*. 2023;51(4): 130-141. DOI: 10.18149/MPM.5142023_12.

Introduction

It is known that various inclusions that in some way have arisen in a homogeneous body affect the local stress-strain state (SSS) of the material in its vicinity [1–3]. This effect can be characterized either by way of the stress concentration coefficients or by way of the parameters used in the destruction mechanics (see, for example, [3–8]).

With laser, plasma and other high-energy methods of concentrated impact on the component, zones of altered structure of the source material appear – the target impact zone and the thermal influence zone surrounding it [9]. In the latter, the structure differs markedly from both the processing zone structure and the structure of the base material, and the management of its properties is limited due to the lack of the possibility of direct influence on the structure formation in this area. Data on the properties of the material in these areas are limited, there are no unambiguous analytical dependencies between their mechanical

characteristics, therefore there is a large uncertainty in their values [10], which is a significant drawback in predicting the behavior of a real object in operating conditions.

Numerous works of domestic and foreign scientists have been devoted to the study of the component properties and SSS during heat treatment by a local highly concentrated heating source [11–20]. In [13] some regularities and interrelations between technological factors determining the features of short-term local thermal impacts and the nature of structural changes and properties of low-alloy steels were established, and in [14] – for steel with reduced calcination of 60RC. In [15], the influence of the laser treatment process on the microstructure peculiarities and the formation of the cast iron thermal influence zone is considered. In the article [16], the influence of heat treatment (annealing, normalization, hardening, tempering) during quenching on the mechanical properties and microstructure of steel ST 37-2 was studied. In [17], a method for assigning surface hardening modes is given, which differs from the known ones in that heat treatment modes are set taking into account not only the specified depth and hardness of the hardened layer, but also the nature of the distribution of the remaining stresses in the material. The article [18] describes a mathematical model for calculating the SSS of elements of composite structures under the impact of a local heating source. In [19] computer simulation of tensile tests of a rod with rectangular zones that have arisen during heat treatment by a moving highly concentrated heat source, the material characteristics of which differ from the properties of the base material, is considered. In [20] for the first time, the analytical method solved the problem of changing the stress-strain state of a polymer material during its orientation extraction.

Instrumental studies conducted by domestic and foreign scientists in the field of sample properties after an exposure to a local heating source are mainly aimed at establishing the nature of structural transformations and hardness of materials [21–25]. The results of studying the mechanical characteristics of the material of the treated zone, in particular, elasticity modules and Poisson coefficients, are not sufficiently presented. Accordingly, the results of studies of the impact of emerging differences in these indicators on the SSS of machine components are not sufficiently represented. Therefore, the issue discussed in the article is relevant.

Materials and Methods

Studies show that the depth of surface hardening is small compared to the thickness of the component, so it is most natural to assess the effect of changes in material parameters for the case when there was no stress gradient in the volume of the untreated material, for example, during axial straining of the sample. Therefore, to assess the degree of influence of the differences in the elasticity module and Poisson coefficient of the zones of the component with unaltered structure compared to the characteristics of the base material, a finite element simulation of the problem of straining a rod with the tracts of the treated material surrounded by an intermediate zone of thermal influence was carried out.

Two cases of track length are considered – a continuous one along the length of the sample and a shortened one (to account for the influence of its butt-end area). The geometry of the zones, the number of tracks and the distances between them varied during the calculations. The length of the shortened section of the track was 5/11 of the length of the selected section of the rod. During heat treatment, depending on the modes, the thickness of the intermediate layer may vary, so the calculations were carried out for different values of this parameter. In view of the symmetry of the problem, the selected quarter of the sample was considered during modeling (Fig. 1).

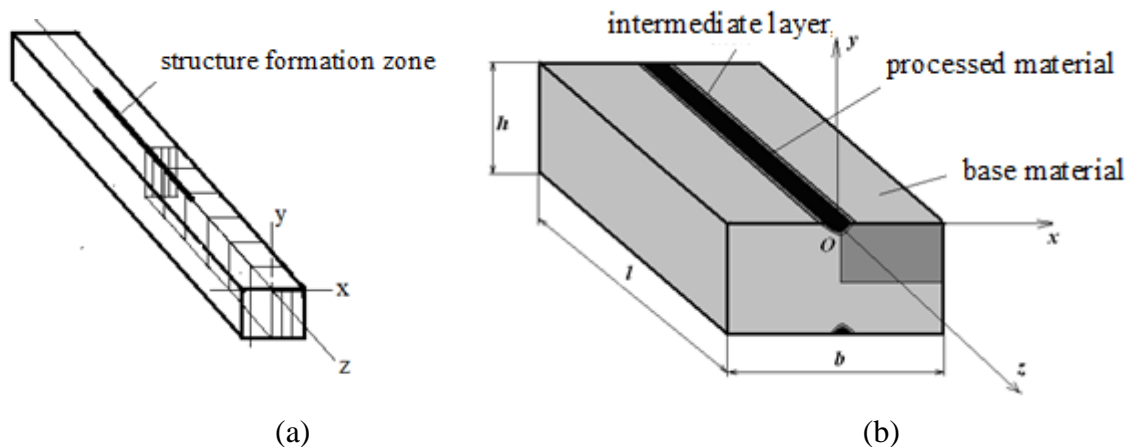


Fig. 1. The sample (a) and the marked element (b)

Two forms of the structure formation zone are analyzed – a rectangular one 0.8×0.4 mm and a crescent-shaped one with a zone of the treated material in the form of a semicircle with a radius of 0.4 mm. The MSC NASTRAN programming complex was used as a calculation package for a model with a rectangular cross-section of the zone, and ANSYS Workbench was used for a crescent-shaped zone.

The finite element model of the sample in the presence of one track is shown in Fig. 2. This volume is comprehensively surrounded by a 0.2 mm thick transition area with a possibility of reducing it to zero. The rest of the volume is occupied by the source (main) material. Overall dimensions of the model are $2.0 \times 2.6 \times 4.4$ mm.

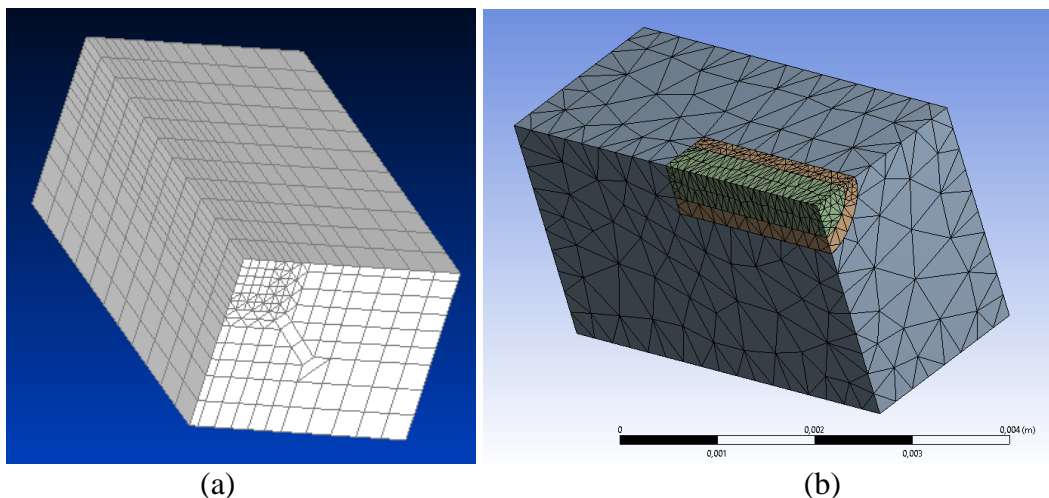


Fig. 2. Finite element models: a) rectangular, b) crescent-shaped

Boundary conditions for displacements were set in the form of a movement restriction in the direction of the axis Oy ($V_y = 0$) at the points of the upper facet of the body, $W_z = 0$ on the rear facet, $U_x = 0$ on the left facet. On the right longitudinal face, boundary conditions of 2 types were set $U_x \neq 0$ (imitation of a rod sample) and $U_x = 0$ (imitation of constrained deformation, which is true, for example, for plates).

The module of elasticity of the initial material was assumed to be equal to $E = E_{bas} = 200$ GPa, the Poisson coefficient $\mu = \mu_{bas} = 0.3$. The elasticity modules of the intermediate and treated layers and their Poisson coefficients varied, but it was assumed that after treatment, the body material at all its points remains in the elastic area of operation, which corresponds to most realizable cases of operation of machine components and mechanisms. SSS in the process of the body cooling directly after heat treatment was not

considered. The indices "bas", "int", "pr" hereafter refer respectively to the source material, the intermediate layer and the treated volume.

Loading was carried out by setting the displacement of the front butt-end section by the value $W_z = 0.0044$ mm, which is determined from the condition of equality of axial stresses $\sigma_z = 200$ MPa for a homogeneous rod. The calculations have shown that the selected rod length is sufficient to equalize the stress state by its volume. The ratio of the elasticity modules of the treated material to the modules of the source material varied within the limits of $K_E = E_{pr}/E_{bas} = 0.8, \dots, 1.5$, Poisson coefficients – within the limits of $K_\mu = \mu_{pr}/\mu_{bas} = 0.7, \dots, 1.4$.

Results and Discussion

A study of the samples SSS with two zones of modified material structure of rectangular and crescent sections for different boundary conditions, the number and size of zones, and material characteristics was carried out. As examples, Figs. 3, 4 show the distributions of equivalent stresses σ_i over the volume of the body for the considered material characteristics and conditions concerning the geometry of treatment. Comparing them, it is possible to determine the direction of change in the material SSS depending on these parameters. The calculated stress values are the average in the corresponding elements. Their values at the angular points of the elements are not used, since due to the small size of the finite elements compared to the overall dimensions of the body, the maximum values in them are quite close to the average. The main stresses σ_I in this problem are close to the longitudinal stresses σ_z .

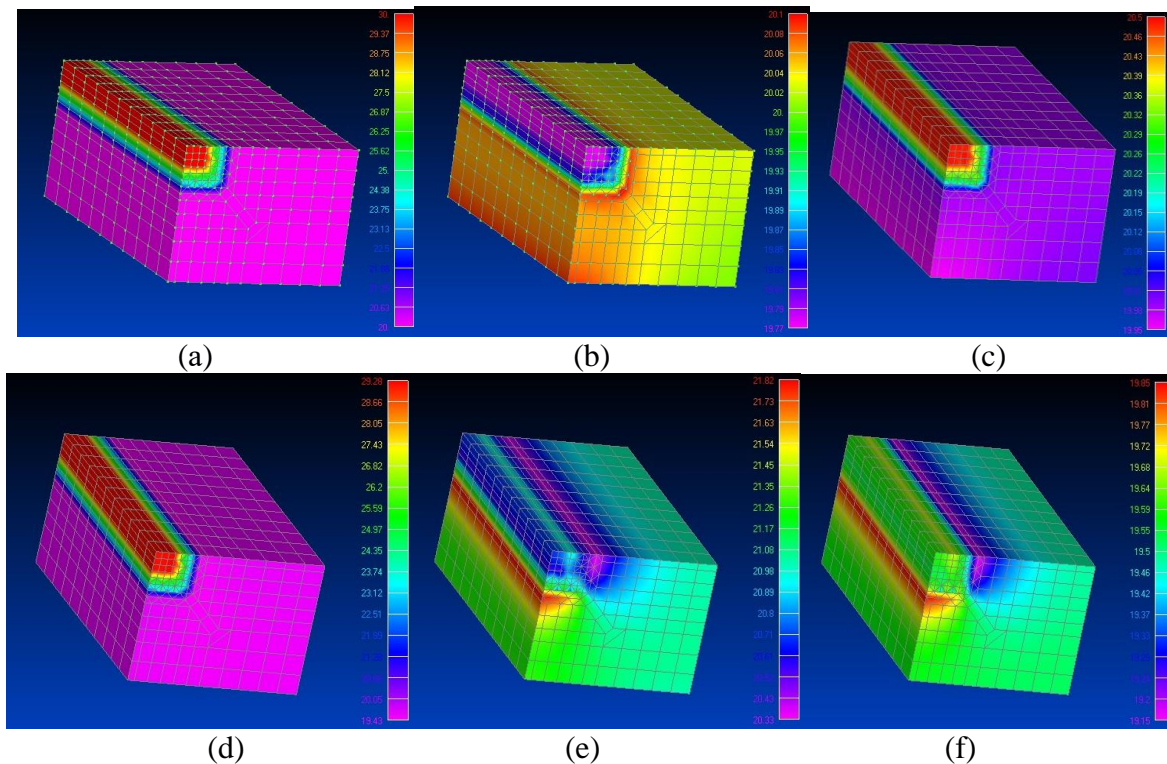


Fig. 3. Distribution of equivalent stresses according to the Mises criterion σ_i for a sample with a rectangular zone [19] with a free (a–c) and a fixed (d–f) right face, thickness of the intermediate layer is 0.2 mm

$$(a, d) E_{bas} = 200 \text{ GPa}, E_{int} = 250 \text{ GPa}, E_{pr} = 300 \text{ GPa}, \mu_{bas} = \mu_{int} = \mu_{pr} = 0.3,$$

$$(b, e) E_{bas} = E_{int} = E_{pr} = 200 \text{ GPa}, \mu_{bas} = 0.3, \mu_{int} = 0.36, \mu_{pr} = 0.42$$

$$(c, f) E_{bas} = E_{int} = E_{pr} = 200 \text{ GPa}, \mu_{bas} = 0.3, \mu_{int} = 0.24, \mu_{pr} = 0.21$$

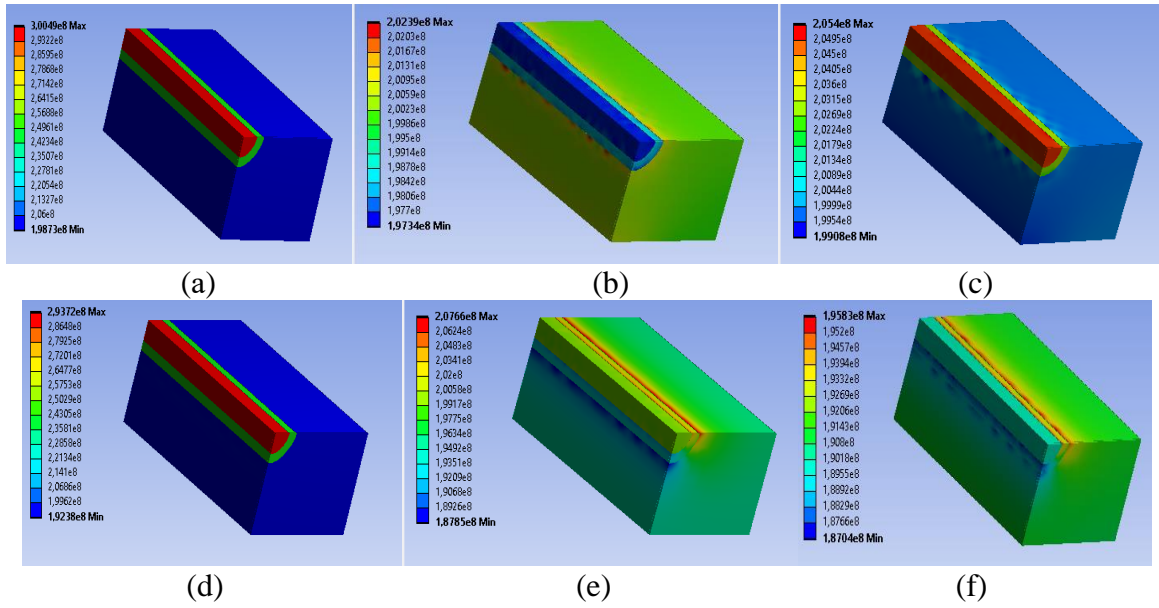


Fig. 4. Distribution of equivalent stresses according to the Mises criterion σ_i for a sample with a crescent-shaped zone with a free (a–c) and a fixed (d–f) right face, thickness of the intermediate layer is 0.2 mm

(a, d) $E_{bas} = 200 \text{ GPa}$, $E_{int} = 250 \text{ GPa}$, $E_{pr} = 300 \text{ GPa}$, $\mu_{bas} = \mu_{int} = \mu_{pr} = 0.3$,

(b, e) $E_{bas} = E_{int} = E_{pr} = 200 \text{ GPa}$, $\mu_{bas} = 0.3$, $\mu_{int} = 0.36$, $\mu_{pr} = 0.42$

(c, f) $E_{bas} = E_{int} = E_{pr} = 200 \text{ GPa}$, $\mu_{bas} = 0.3$, $\mu_{int} = 0.24$, $\mu_{pr} = 0.21$

The results of the calculations show that any deviation from the initial parameters leads to a change in the stress distribution over the volume of the part. Their maximum can be realized both in the processed layer, and in the main material, intermediate layer or at the boundaries of layers. For the shortened zone, the greatest stresses occur in the area of the treated material adjacent to the main one. When the modulus of elasticity of the treated layer increases over the modulus of the initial material, there is always an increase in the maximum stresses σ_i and σ_z , while the minimum σ_i and σ_z arising at the boundary of the transition zone and the base material do not obey this pattern. When the modulus of elasticity of the treated zone decreases with respect to the modulus of elasticity of the base material, the stress concentration occurs in the base material, as a result of which the maximum stresses are close to the nominal ones. The main difference for the crescent-shaped zones is that the maximum stress occurs on the axis of symmetry of the segment.

It is established that the influence of Poisson coefficient on the stresses is nonlinear. Its deviation for the treated zone from the coefficient for the initial (base) material in any direction leads to an increase in maximum stresses, but it can affect the minimum level in different ways. The results of the research are presented by the graphs in Figs. 4, 5. When Poisson coefficient of the source material changes, the structures in these figures will also change in a certain way. These observations regarding the influence of Poisson coefficients correspond to [1, pp. 546-573].

Figures 5-9 show the values of the ratios σ_z^{\max} to the reference value $\sigma_z = 200 \text{ MPa}$, which represent the stress concentration coefficients for this problem $K_\sigma = \sigma_z^{\max} / \sigma_z$, depending on the ratios of the material parameters $K_E = E_{pr} / E_{bas}$ or $K_\mu = \mu_{pr} / \mu_{bas}$. Figures 4 and 5 illustrate the case of a rectangular-shaped zone of the structure formation, Figs. 6-8 – the case of a crescent-shaped one. Light signs relate to the case of a free right facet $U_x \neq 0$ (the

case of the rod), and the dark ones – to the case of a fixed facet $U_x = 0$ (constrained deformation).

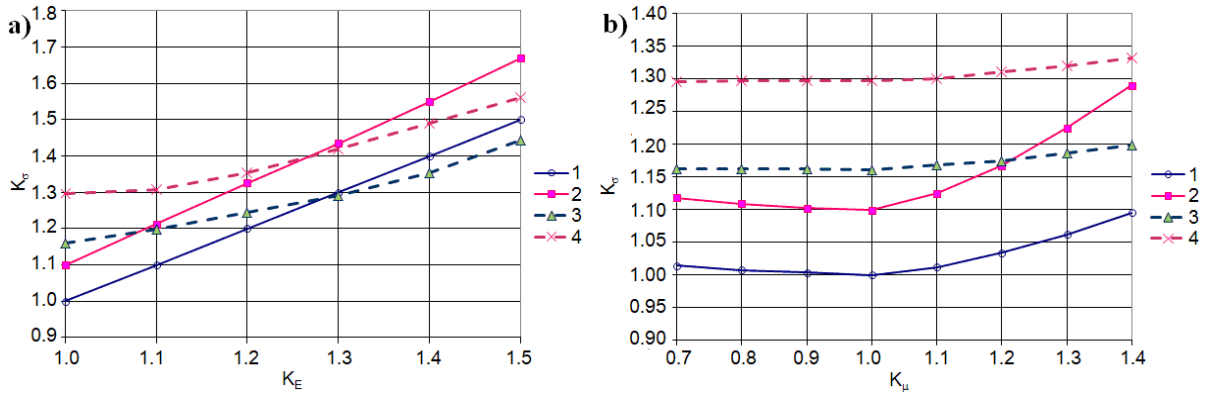


Fig. 5. Influence of elasticity module (a) and Poisson coefficient (b) on longitudinal stresses; intermediate layer is 0.2 mm thick:
 1 – long zone, free right facet; 2 – long zone, fixed right facet;
 3 – shortened zone, free right facet; 4 – shortened zone, fixed right facet

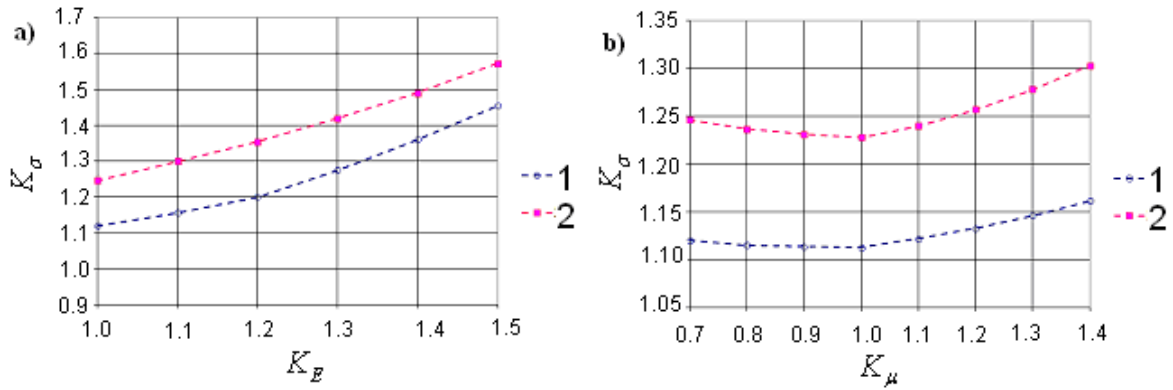


Fig. 6. Influence of the elasticity module (a) and Poisson coefficient (b) on longitudinal stresses in a shortened track with an intermediate layer 0.1 mm thick:
 1 – free right facet, 2 – fixed right facet

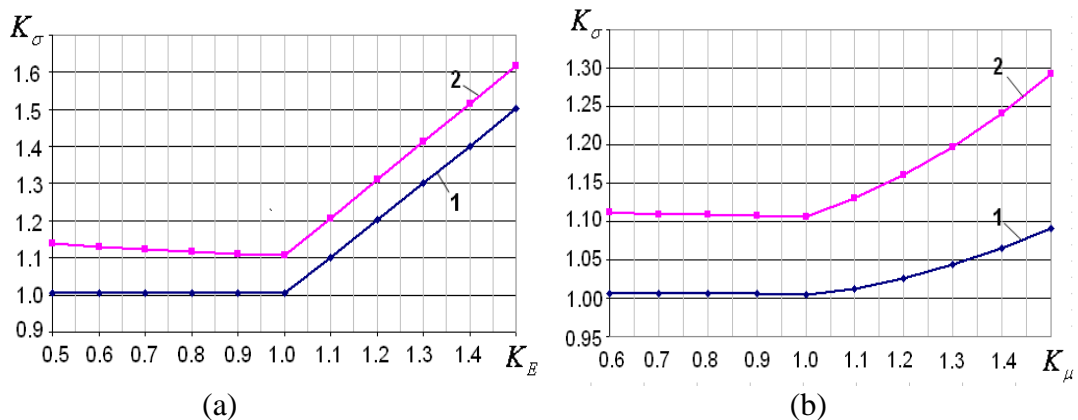


Fig. 7. Dependence of the stress concentration coefficient on K_E (a) and K_μ (b) for a sample with a crescent-shaped zone along the entire length:
 1 – rod pattern (right facet is free), 2 – constrained deformation (right facet is fixed)

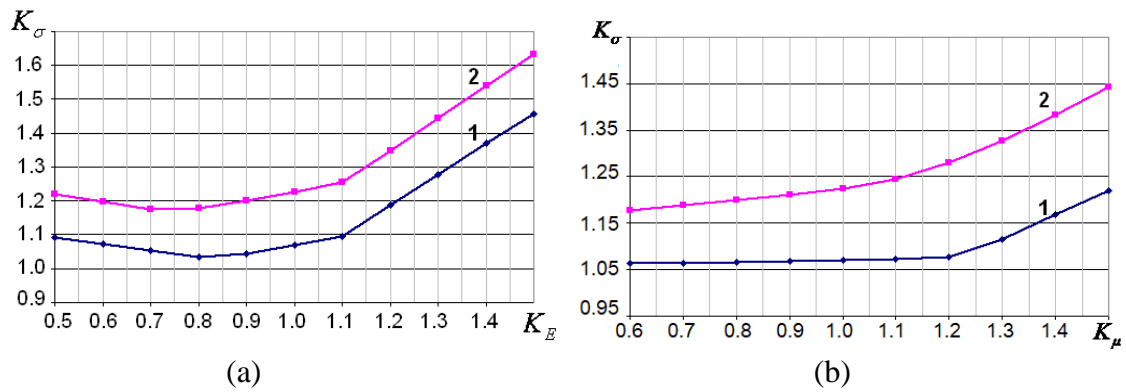


Fig. 8. Dependence of the stress concentration coefficient on K_E (a) and K_μ (b) for a sample with a shortened crescent-shaped track:
1 – rod sample (right facet is free), 2 – constrained deformation (right facet is fixed)

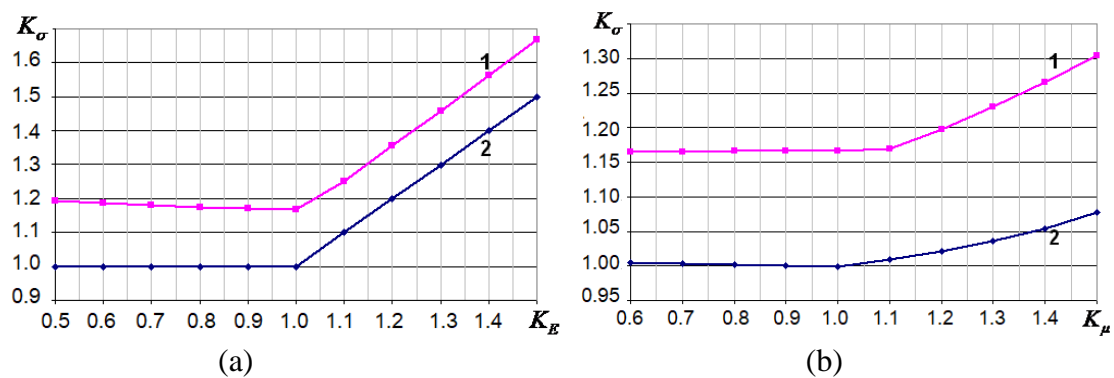


Fig. 9. Dependence of the stress concentration coefficient K_E (a) and K_μ (b) for samples with two crescent-shaped track along the entire length and the distance between them $\delta = 0.4$ mm:
1 – rod sample (right facet is free), 2 – constrained deformation (right facet is fixed)

In the case of constrained deformation, the stresses in all the cases considered are higher than in the case of free deformation. The stress concentration coefficients for the rectangular and crescent-shaped zones of the altered structure differ insignificantly, but the values for the rectangular zone are higher.

For a diagram with a shortened track, when reducing the intermediate layer thickness to zero, a change in Poisson coefficient relative to the value for the source material leads to a slight decrease in stress concentration.

The case of the presence of three parallel tracks along the entire length of the sample, arranged symmetrically at distances $\delta = 0.0-0.6$ mm from each other, is also considered. As an example for a rectangular track, Figs. 10-13 show the distribution of equivalent stresses σ_i according to Mises for the case when the distance between the roads is 0, 0.1 and 0.6 mm.

The research results and their comparison with the data given in [20] for $\delta = 0.2$ mm show an insignificant effect of the distance δ on the stress concentration factor. Therefore the influence of mechanical and geometric parameters change of materials on the SSS of the body when exposed to a high-energy jet can be carried out based on the results of calculations for a single track. The difference in results does not exceed several percent. A variation in the distance between the tracks for a crescent-shaped zone of structure formation does not affect the values of the stress concentration coefficient, either.

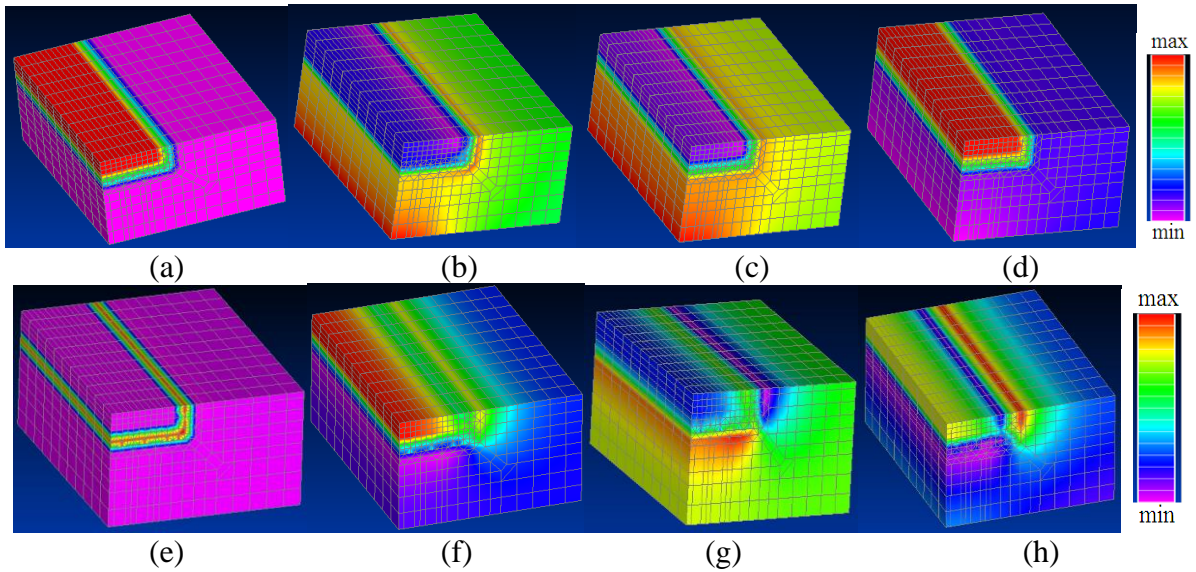


Fig. 10. Distribution of equivalent stresses according to Mises σ_i with a free (a–d) and fixed (e–h) right facet ($\delta = 0$ mm, rectangular-shaped zone):

(a, e) $E_{bas} = 200$ GPa, $E_{int} = 250$ GPa, $E_{pr} = 300$ GPa, $\mu_{bas} = \mu_{int} = \mu_{pr} = 0.3$

(b, f) $E_{bas} = E_{int} = E_{pr} = 200$ GPa, $\mu_{bas} = 0.3$, $\mu_{int} = 0.36$, $\mu_{pr} = 0.42$

(c, g) $E_{bas} = E_{int} = E_{pr} = 200$ GPa, $\mu_{bas} = 0.3$, $\mu_{int} = 0.24$, $\mu_{pr} = 0.21$

(d, h) $E_{bas} = E_{int} = E_{pr} = 200$ GPa, $\mu_{bas} = 0.21$, $\mu_{int} = 0.24$, $\mu_{pr} = 0.3$

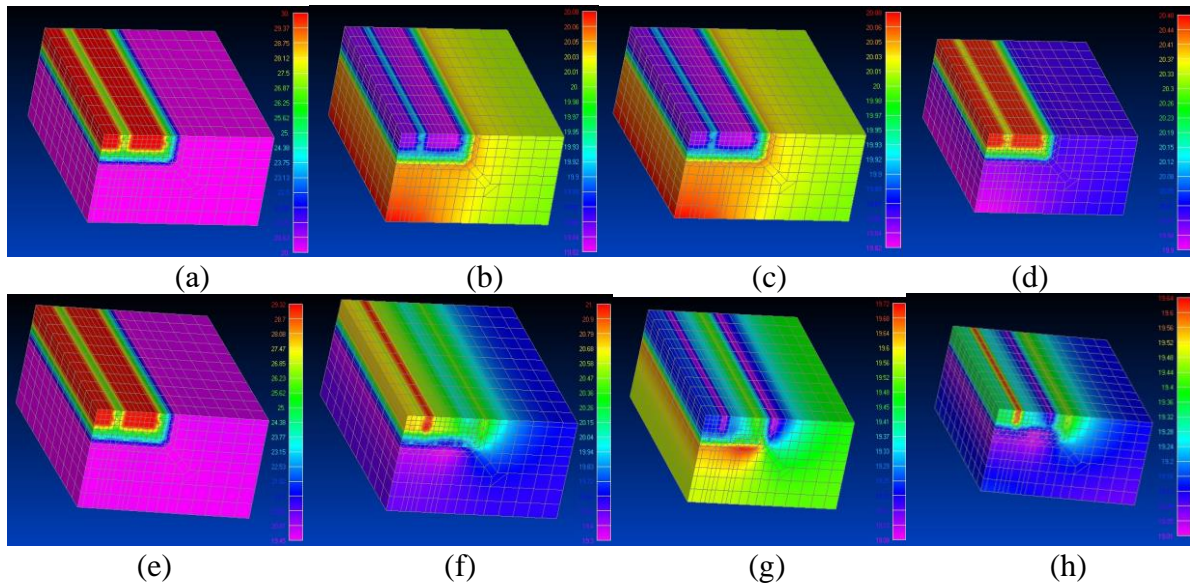


Fig. 11. Distribution of equivalent stresses according to Mises σ_i with a free (a–d) and fixed (e–h) right facet ($\delta = 0.1$ mm, rectangular-shaped zone):

(a, e) $E_{bas} = 200$ GPa, $E_{int} = 250$ GPa, $E_{pr} = 300$ GPa, $\mu_{bas} = \mu_{int} = \mu_{pr} = 0.3$

(b, f) $E_{bas} = E_{int} = E_{pr} = 200$ GPa, $\mu_{bas} = 0.3$, $\mu_{int} = 0.36$, $\mu_{pr} = 0.42$

(c, g) $E_{bas} = E_{int} = E_{pr} = 200$ GPa, $\mu_{bas} = 0.3$, $\mu_{int} = 0.24$, $\mu_{pr} = 0.21$

(d, h) $E_{bas} = E_{int} = E_{pr} = 200$ GPa, $\mu_{bas} = 0.21$, $\mu_{int} = 0.24$, $\mu_{pr} = 0.3$

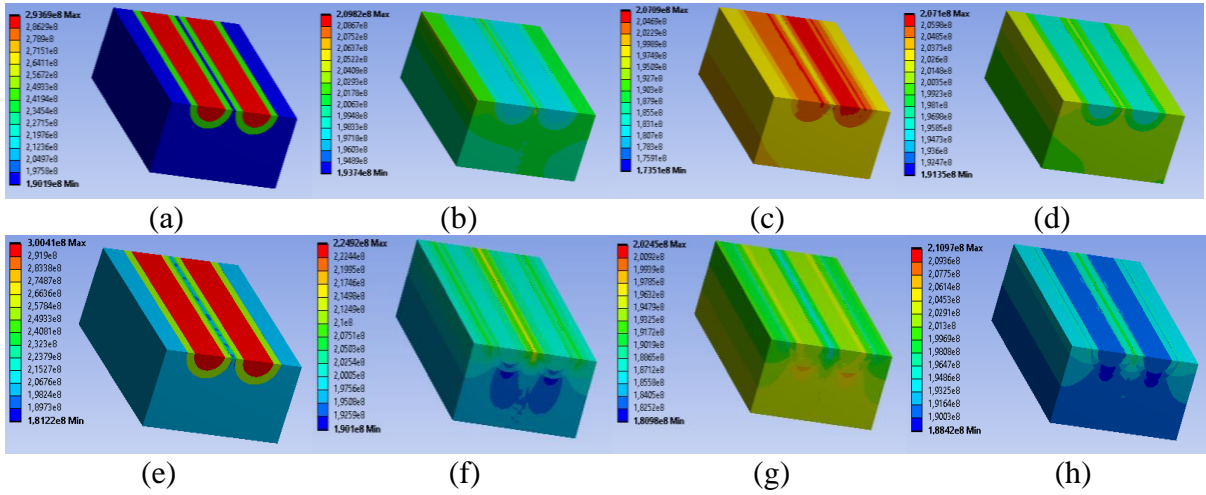


Fig. 12. Distribution of equivalent stresses according to Mises σ_i with a free (a–d) and fixed (e–h) right facet ($\delta = 0.1$ mm, crescent-shaped zone):

- (a, e) $E_{bas} = 200$ GPa, $E_{int} = 250$ GPa, $E_{pr} = 300$ GPa, $\mu_{bas} = \mu_{int} = \mu_{pr} = 0.3$
 (b, f) $E_{bas} = E_{int} = E_{pr} = 200$ GPa, $\mu_{bas} = 0.3$, $\mu_{int} = 0.36$, $\mu_{pr} = 0.42$
 (c, g) $E_{bas} = E_{int} = E_{pr} = 200$ GPa, $\mu_{bas} = 0.3$, $\mu_{int} = 0.24$, $\mu_{pr} = 0.21$
 (d, h) $E_{bas} = E_{int} = E_{pr} = 200$ GPa, $\mu_{bas} = 0.21$, $\mu_{int} = 0.24$, $\mu_{pr} = 0.3$

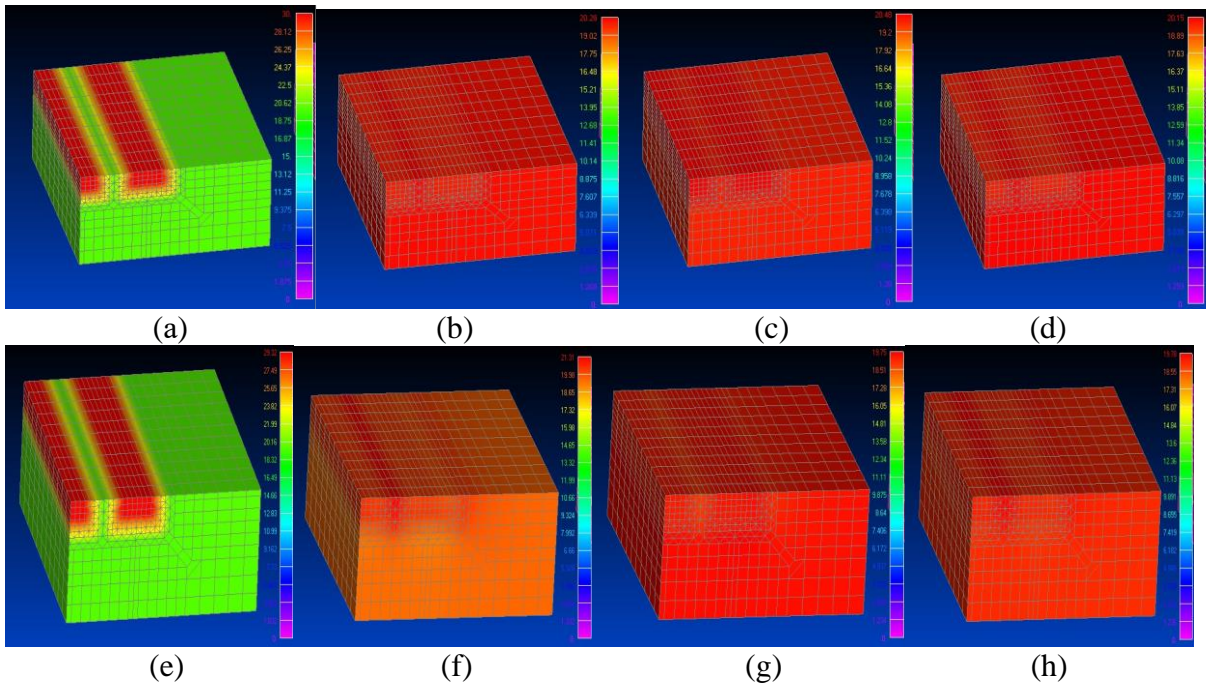


Fig. 13. Distribution of equivalent stresses according to Mises σ_i with a free (a–d) and fixed (e–h) right facet ($\delta = 0.6$ mm, rectangular-shaped zone):

- (a, e) $E_{bas} = 200$ GPa, $E_{int} = 250$ GPa, $E_{pr} = 300$ GPa, $\mu_{bas} = \mu_{int} = \mu_{pr} = 0.3$
 (b, f) $E_{bas} = E_{int} = E_{pr} = 200$ GPa, $\mu_{bas} = 0.3$, $\mu_{int} = 0.36$, $\mu_{pr} = 0.42$
 (c, g) $E_{bas} = E_{int} = E_{pr} = 200$ GPa, $\mu_{bas} = 0.3$, $\mu_{int} = 0.24$, $\mu_{pr} = 0.21$
 (d, h) $E_{bas} = E_{int} = E_{pr} = 200$ GPa, $\mu_{bas} = 0.21$, $\mu_{int} = 0.24$, $\mu_{pr} = 0.3$

It was found that with an increase in δ , the change in the Poisson's ratio of the zones of the modified structure in any direction with respect to the value for the base material practically does not affect the equivalent stresses (Fig. 13).

Transverse stresses σ_x arising during loading depend on geometric conditions and differences in the parameters E and μ , increasing with the growth of ratios E_{pr}/E_{bas} and μ_{pr}/μ_{bas} . The main role is played by the presence constraint of deformation.

In its absence ($U_x = \text{var}$), the stresses are insignificant, vary from zero to several MPa units and can arise both in the treated layer itself and under it at the boundary with the base material. If there are several tracks σ_x in the treated layer, they can be both positive ($\mu_{pr}/\mu_{bas} > 1$) and negative ($\mu_{pr}/\mu_{bas} < 1$) regardless of the distance between the tracks. Their maximum level in the calculations was 3.82 MPa.

If $U_x = 0$, then the stresses σ_x in the treated layer are tensile. At $\mu_{pr}/\mu_{bas} < 1$ they are slightly below the level $\sigma_z/3$, but they increase at $\mu_{pr}/\mu_{bas} > 1$ while remaining below the value $\sigma_z/2$. In case of several tracks, their maximum depends on the distance between them ($\delta = 0.2$ mm, $\sigma_{max} = 11.82$ MPa at $\sigma_z = 25.42$ MPa, $\mu_{pr} = 0.42$).

The levels of transverse stresses σ_x for samples with a crescent-shaped structure formation both qualitatively and quantitatively correspond to the case of a rectangular zone and are shown in Fig. 14.

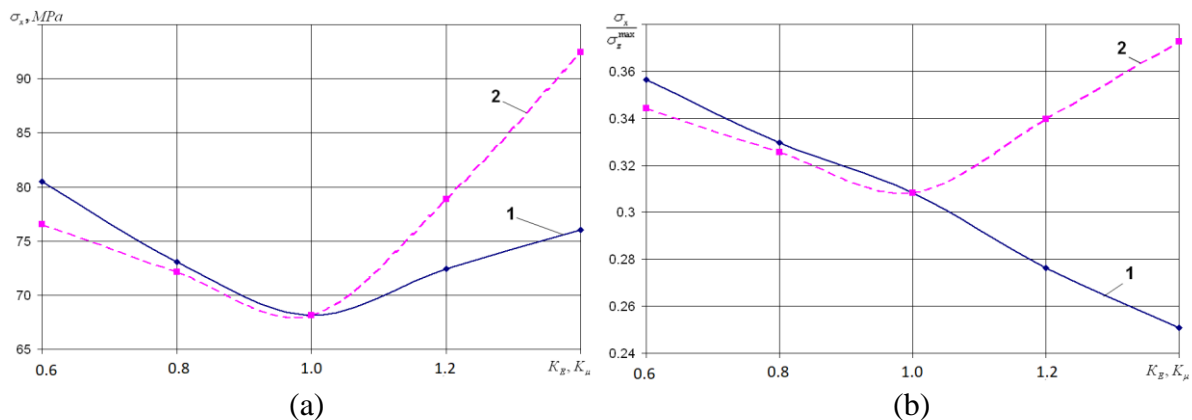


Fig. 14. Dependence of transverse stresses σ_x (a) and their relations to the maximum longitudinal stresses (b) for the case of a sickle-shaped track at $E=\text{var}$ (1) and $\mu=\text{var}$ (2)

Conclusion

The influence of the characteristics of the zones of the altered structure of the source material arising after the heat treatment of samples by a moving highly concentrated heat source on the stress-strain state under tension has been studied. Two forms of the zone of structure formation are considered – rectangular and crescent. Based on the results of finite element calculation in a wide range of values of the elasticity module and Poisson coefficient, the SSS of samples with one or more zones of the material altered structure along its entire length and on the part of the length was determined. Stress concentration coefficients in the vicinity of treatment zones for various boundary conditions, sizes of zones and distances between them are determined. An insignificant influence of the distance between the tracks on the stress concentration coefficient has been established. Transverse stresses depending on the mechanical characteristics of the treated and source material have been investigated.

The obtained values of the concentration coefficients, although they reflect the general trends of SSS transformation in the presence of local material treatment, are not

unambiguous, but depend on geometric and mechanical characteristics of an object (the relations of the treated zone sizes and the initial component, the thickness of the intermediate layer, elasticity modules and Poisson coefficients of the layer materials).

The research results show both the importance of knowing the exact values of the material mechanical characteristics in the field of local impact, and the necessity of carrying out calculations for the hardened part, taking into account the presence of this impact, without which it is impossible to choose an optimal treatment mode for ensuring the required product performance qualities.

References


1. Muskhelishvili NI. *Some basic problems of the mathematical theory of elasticity*. Moscow: Science; 1966. (In-Russian)
2. Neiber G. *Stress concentration*. Moscow: Gostekhizdat; 1947.
3. Savin GN. *Stress concentration near holes*. Moscow: State Publishing House of technology-theoretical lit.; 1951. (In-Russian)
4. Birger IA, Panovko YG. (ed.) *Strength, stability, vibrations*. Moscow: Mechanical Engineering. 1968. p.463. (In-Russian)
5. Peterson R. *Stress concentration coefficients. Graphs and formulas for calculating structural elements for strength*. Moscow: World; 1977. (In-Russian)
6. Ito Y, Murakami Y, Hasebe N. *Handbook of stress intensity coefficients*. Moscow: World; 1990.
7. Cherepanov GP. *Mechanics of brittle fracture*. Moscow: Science; 1974. (In-Russian)
8. Berezhnitsky LT, Delyavsky MV, Panasyuk VV. *Bending of thin plates with crack-type defects*. Kiev: Scientific Thoughts; 1979. (In-Russian)
9. Grigoriev SN, Ivannikov AY, Prozhega MV, Zakharov IN, Kuznetsova OG, Levin AM. The influence of the highly concentrated energy treatments on the structure and properties of medium carbon steel. *Metals*. 2020;10(12): 1669.
10. Gulyaev AP. *Metallovedenie*. Moscow: Book on demand; 2020. (In-Russian)
11. Dinesh BP, Balasubramanian KR, Buvanashakaran GH. Laser surface hardening. *International Journal of Surface Science and Engineering*. 2011;5(2/3): 131-151.
12. Bely AV, Makushok EM, Pobol IL. *Surface hardening treatment with the use of concentrated energy flows*. Minsk: Science and technology; 1990. (In-Russian)
13. Sharapova DM. *Evolution of structure and properties of structural low-alloy steels under short-term local thermal effects by concentrated heat sources. Dissertation of the PhD of Technical Sciences*. St. Petersburg, 2018. (In-Russian)
14. Gordienko AI, Michluk AI, Ivashko VV, Vegera II The influence of heating modes on the structure and mechanical properties of 60PP steel. *Casting and Metallurgy*. 2011;1(59): 146-153.
15. Voitovich ON, Sokolov IN. Investigation of the influence of laser heat treatment parameters on the properties of hardened surface layers. *Bulletin of the Belarusian-Russian University*. 2013;2: 6-14.
16. Fadara TG, Akanbi OY, Fadare DA. Effect of heat treatment on mechanical properties and microstructure of NST 37-2 steel. *Journal of Minerals & Materials Characterization & Engineering*. 2011;10(3): 299-308.
17. Ivantsievsky VV. *Control of the structural and stressed state of the surface layers of machine parts during their hardening using concentrated sources of heating and finishing grinding. Dissertation of the Doctor of Technical Sciences*. Novosibirsk; 2012. (In-Russian)
18. Gulakov SV, Shcherbakov SV, Zavarika NG. Computer modeling of the stress-strain state of elements of composite structures under the influence of a local heating source. *Bulletin of Pryazovsky State Technical University*. 2004;14: 223-226.

19. Verameichyk AI, Neroda MV, Holodar' BG. Konechno-elementnoe modelirovanie zadachi o rastyazhenii materiala s zonami izmenennoj struktury. *Mekhanika mashin, mekhanizmov i materialov*. 2022;3(60): 77–84. (In-Russian)
20. Skyba MY, Synyuk OM, Zlotenko BM. Model of changing the stressed-deformed state of a polymer sheet during stretching. *Scientific Bulletin of National Mining University*. 2019;1: 83-89.
21. Tkacheva AV, Abashkin EE. Impact of forced cooling of the joint zone and thermal effect on the distribution values of residual stress generated by arc welding. *Materials Physics and Mechanics*. 2022;50(3): 509-517.
22. Dowden J, Schulz W. The Theory of Laser Materials Processing. In: *Heat and Mass Transfer in Modern Technology*. Springer; 2017.
23. Ruzankina JS, Vasiliev O, Tarasov S. Investigation of functional properties of metal surfaces after laser treatment. *Journal of Physics: Conference Series*. 2019;1410: 012171.
24. Bartkowska A, Kuklinski M, Kieruj P. The influence of laser heat treatment on the geometric structure of the surface and condition of the surface layer and selected properties of Waspaloy. *MATEC Web of Conferences*. 2017;121: 03006.
25. Muthukumaran G, Dinesh Babu P. Laser transformation hardening of various steel grades using different laser types. *Journal of the Brazilian Society of Mechanical Sciences and Engineering*. 2021;43(2): 103.

THE AUTHORS

Verameichyk A.I. 
e-mail: vai_mrtm@bstu.by

Neroda M.V. 
e-mail: nerodamv@mail.ru

Holodar B.G. 
e-mail: hbg@list.ru